Eur. Phys. J. A (2012) **48**: 105
DOI 10.1140/epja/i2012-12105-7

THE EUROPEAN PHYSICAL JOURNAL A

Regular Article – Experimental Physics

Coulomb excitation of ^{107}Sn

D.D. DiJulio[1,a], J. Cederkall[1], C. Fahlander[1], A. Ekström[2], M. Hjorth-Jensen[2,3], M. Albers[4,b], V. Bildstein[5,c], A. Blazhev[4], I. Darby[6], T. Davinson[7], H. De Witte[6], J. Diriken[6,8], Ch. Fransen[4], K. Geibel[4], R. Gernhäuser[5], A. Görgen[9], H. Hess[4], J. Iwanicki[10], R. Lutter[11], P. Reiter[4], M. Scheck[12,d], M. Seidlitz[4], S. Siem[9], J. Taprogge[4], G.M. Tveten[9], J. Van de Walle[13], D. Voulot[14], N. Warr[4], F. Wenander[14], and K. Wimmer[5,e]

[1] Physics Department, Lund University, Box 118, SE-221 00 Lund, Sweden
[2] Department of Physics and Center of Mathematics for Applications, University of Oslo, N-0316, Oslo, Norway
[3] National Superconducting Cyclotron Laboratory and Department of Physics and Astronomy, Michigan State University, East Lansing, MI 48824, USA
[4] Institute of Nuclear Physics, University of Cologne, D-50937 Cologne, Germany
[5] Physik Department E12, Technische Universität München, D-85748 Garching, Germany
[6] Instituut voor Kern- en Stralingsfysica, KU Leuven, Celestijnenlaan 200D, B-3001 Leuven, Belgium
[7] Department of Physics and Astronomy, University of Edinburgh, UK
[8] Studiecentrum voor Kernenergie/Centre d'Etude de l'énergie Nucléaire (SCK CEN), B-2400 Mol, Belgium
[9] Department of Physics, University of Oslo, Norway
[10] Heavy Ion Laboratory, University of Warsaw, Poland
[11] Fakultät für Physik, Ludwig-Maximilians-Universität München, D-85748 Garching, Germany
[12] Oliver Lodge Laboratory, University of Liverpool, United Kingdom
[13] PH Department, CERN 1211, Geneva 23, Switzerland
[14] AB Department, CERN 1211, Geneva 23, Switzerland

Received: 23 April 2012 / Revised: 19 June 2012
Published online: 30 July 2012
© The Author(s) 2012. This article is published with open access at Springerlink.com
Communicated by R. Krücken

Abstract. The radioactive isotope ^{107}Sn was studied using Coulomb excitation at the REX-ISOLDE facility at CERN. This is the lightest odd-Sn nucleus examined using this technique. The reduced transition probability of the lowest-lying $3/2^+$ state was measured and is compared to shell-model predictions based on several sets of single-neutron energies relative to ^{100}Sn. Similar to the transition probabilities for the 2^+ states in the neutron-deficient even-even Sn nuclei, the measured value is underestimated by shell-model calculations. Part of the strength may be recovered by considering the ordering of the $d_{5/2}$ and $g_{7/2}$ single-neutron states.

1 Introduction

In recent years, Coulomb excitation measurements of the neutron-deficient even-even Sn nuclei have revealed $\sim 30\%$ enhanced transition probabilities for the first excited 2^+ states compared to state-of-the-art shell-model calculations [1–4]. It is of interest to see if this trend is also observed for transition probabilities in the neutron-deficient odd-Sn isotopes. Relatively little work has been carried out using Coulomb excitation in these isotopes. Prior to this study, the lightest odd-Sn nucleus studied was ^{115}Sn [5].

Coulomb excitation measurements favor the population of excited states built upon collective excitations over excited states built upon single-particle excitations. Such a measurement therefore makes it possible to identify excited states which are likely to be of single-particle character. In the light Sn nuclei, the excited states can be interpreted as arising from the excitation of neutrons outside of a ^{100}Sn core. As a direct measurement of the single-neutron states in ^{101}Sn is currently out of reach, an alternative approach is to identify these states in the heavier Sn nuclei and study their migration across the Sn isotopic chain. The five single-neutron orbits of interest are

[a] e-mail: douglas.dijulio@nuclear.lu.se
[b] *Present address*: Physics Division, Argonne National Laboratory, Argonne, Illinois 60439, USA.
[c] *Present address*: Department of Physics, University of Guelph, Guelph, Ontario NIG 2W1, Canada.
[d] *Present address*: Institut für Kernphysik, Technische Universität Darmstadt, D-64289 Darmstadt, Germany.
[e] *Present address*: National Superconducting Cyclotron Laboratory, Michigan State University, East Lansing, MI 48824, USA.

the $d_{5/2}, g_{7/2}, s_{1/2}, d_{3/2}$ and $h_{11/2}$ orbits. The only firm experimental evidence for these orbits in ^{101}Sn is the energy spacing between the $d_{5/2}$ and $g_{7/2}$ orbits, measured to be 172 keV [6,7]. The lightest of the odd-Sn isotopes with well-established candidates built upon each of the five neutron orbits is ^{111}Sn. The spectroscopic strengths for these states have been reported in a number of reaction studies [8]. No such data is currently available for the lighter Sn nuclei. It should be mentioned that the states referred to as single-neutron states are those which carry the largest single-neutron component. In ^{109}Sn, there is conflicting evidence for the location of the $s_{1/2}$ orbit. β-decay measurements suggest that a level at 545 keV could be this state [9]. However, a previous study using the ^{106}Cd$(\alpha, p\gamma)^{109}$Sn reaction suggested a $3/2^+$ spin for this level based on angular distribution measurements [10]. As discussed in ref. [9], no conclusive candidate for the $s_{1/2}$ state has been identified in ^{107}Sn.

In this work, we present results of Coulomb excitation measurements of the nucleus ^{107}Sn. This is the first such measurement in which the reduced transition probability, $B(E2; 5/2_1^+ \rightarrow 3/2_1^+)$ value, for the lowest-lying $3/2^+$ state has been measured. Similar to the neutron-deficient even-even Sn nuclei, the value is enhanced with respect to shell-model predictions. Part of the strength can be recovered by considering the ordering of the low-lying $d_{5/2}$ and $g_{7/2}$ orbits, which has been recently debated [6, 7]. The ordering of these orbits may also be important for the even-even Sn nuclei. The three higher-lying orbits may in addition contribute to some extent to the increased strength. In a recent study, the $s_{1/2}$ orbit has been suggested to be responsible for the recently observed loss of collectivity in the transition strengths of the even-even Sn nuclei around midshell [11].

2 Experimental methods

The Coulomb excitation experiment was carried out at the REX-ISOLDE [12] facility at CERN. The ^{107}Sn radioactive beam was produced by bombarding a 27 g/cm^2 LaC_x target by a 1.4 GeV proton beam delivered by the PS Booster with an intensity of $\sim 3.3 \times 10^{13}$ protons/pulse (15–18 pulses/min). The Sn atoms diffused through the target material and effused into a transfer cavity where they were singly ionized using three-step laser ionization. Elements with a low ionization potential were also surface ionized in the transfer cavity and were electromagnetically extracted along with the Sn atoms. The general purpose separator of the facility was used to select a beam with mass number $A = 107$. The isobaric beam was continuously delivered to REX-TRAP [13] where the ions were cooled, bunched, and transferred to the electron beam ion source (EBIS) [14]. The ions were charge bred for 59 ms to a charge state of 26^+ and further separated according to their A/q ratio prior to injection into the REX linear accelerator. The final energy of the beam was 2.87 MeV/u after acceleration and before hitting the 1.95 mg/cm^2 99.93% isotopically enriched ^{58}Ni target.

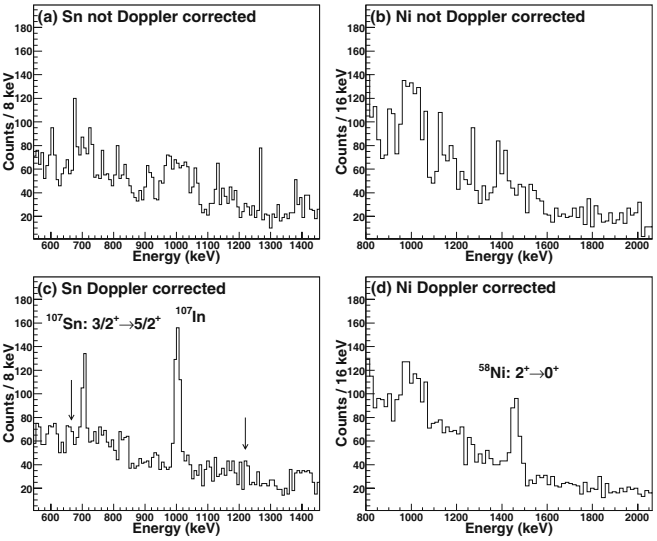

Fig. 1. The γ-ray spectra collected during the experiment without Doppler correction gated on (a) Sn and (b) Ni and with Doppler correction gated on (c) Sn and (d) Ni. The peak labeled ^{107}In arises from the Coulomb excitation of the isobaric beam contaminant. The two arrows indicate the possible presence of two other decays in ^{107}Sn.

The emitted γ-rays, after Coulomb excitation, were detected with the MINIBALL detector array [15]. The array consisted of a set of Ge detector clusters, positioned in a close geometry, surrounding the target position. Each Ge cluster contained three HPGe crystals that were six-fold segmented. The scattered and ejected particles were detected in a double-sided silicon strip detector (DSSSD) located downstream from the target [16]. The DSSSD was divided into four quadrants, each with 16 annular strips (front face) and 24 radial strips (back face) coupled pairwise. The collected data consisted of both events in which one particle was detected (1p events) in the DSSSD and events where both the recoil and scattered particle (2p events) were detected. Due to the kinematics of the reaction, the scattered Ni and Sn particles could be uniquely identified by the DSSSD. The segmentation provided by the DSSSD made it possible to reconstruct the energies and angles of the not detected particles in the 1p event data set using the two-body kinematics of the reaction. The combined 1p events + reconstructed particle and 2p events make up the data analyzed in this work.

3 Experimental results and analysis

The collected spectra from the experiment with and without Doppler correction are shown in fig. 1 and the extracted peak areas and relative intensities used in the analysis are presented in table 1. The data corresponds to γ-rays in coincidence with scattered Ni particles between 28.6° and 46.0°. A γ-ray, resulting from the $3/2_1^+ \rightarrow 5/2_1^+$ transition at 704 keV [17] is clearly seen in fig. 1c. The known level scheme for ^{107}Sn is shown on the left side

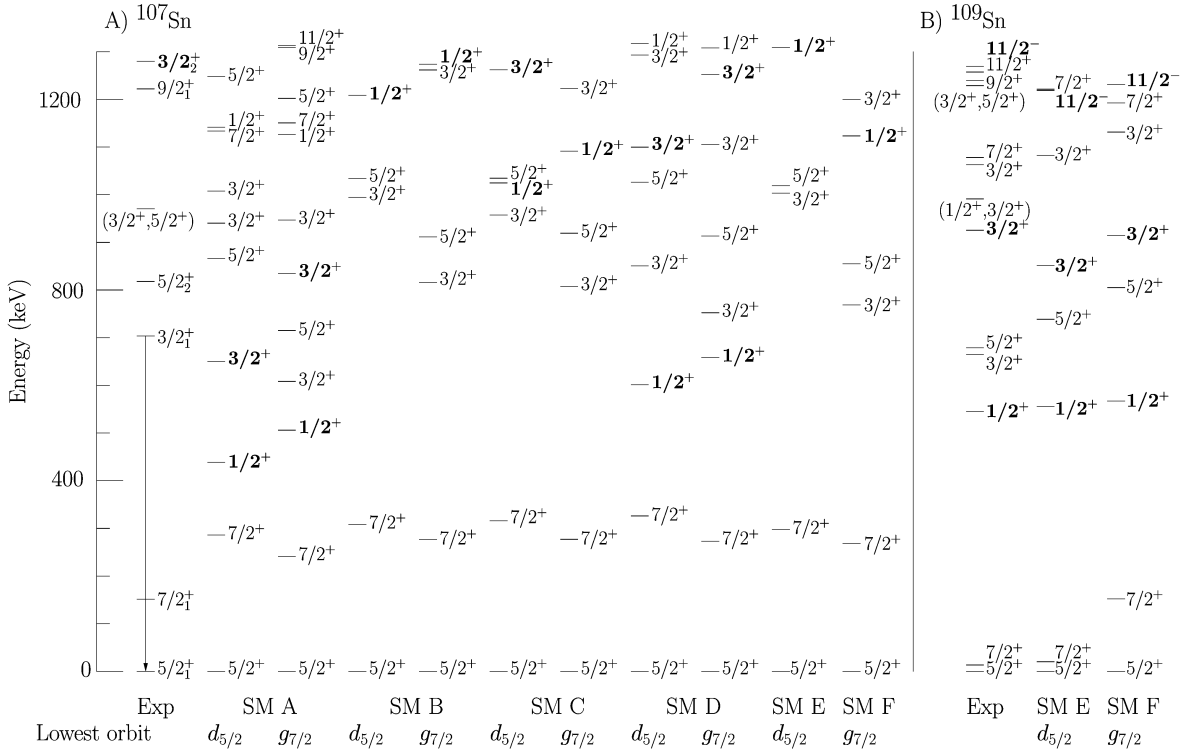

Fig. 2. The experimental and calculated excited states for A) ^{107}Sn and B) ^{109}Sn. The experimental energies are taken from refs. [17,24]. The arrow corresponds to the observed 704 keV $3/2_1^+ \rightarrow 5/2_1^+$ transition. The bold markers indicate the single-neutron states as discussed in the text. The calculations correspond to the different sets of single-neutron orbits given in table 2 for both choices of ground states in ^{101}Sn.

Table 1. Measured peak areas, relative intensities, and the extracted reduced transition probability. Energies taken from refs. [17,18].

Transition	E_γ (keV)	Area	Rel. Int.
Sn $3/2_1^+ \rightarrow 5/2_1^+$	704	140(20)	1.92(28)
Sn $5/2_2^+ \rightarrow 7/2_1^+$	667	< 71	< 0.94
Sn $9/2_1^+ \rightarrow 5/2_1^+$	1222	< 66	< 1.27
Ni $2^+ \rightarrow 0^+$	1454	47(11)[a]	1.00(24)[a]
$B(E2; 5/2_1^+ \rightarrow 3/2_1^+)$	$0.045^{+0.023}_{-0.017}$	e^2b^2	

[a] Peak area and intensity due to the excitation of Sn particles, determined using the beam purity and the area under the peak shown in fig. 1d.

of fig. 2 [17] for reference. The γ-ray at 1001 keV in the Sn Doppler corrected spectrum can be attributed to the Coulomb excitation of the isobaric beam contaminant ^{107}In [17]. The contaminant structure is also present when the laser ionization is switched off, while the Sn peak disappears. The amount of isobaric contaminant in the beam was determined by running alternating cycles of beam pulses with the laser on and off. The Sn fraction in the beam, with the laser ionization switched on, was calculated to be 31(6)% from the number of counts in the observed ^{107}In peak and the number of particles in the DSSSD from the laser on and off runs. The intensity of the Sn beam was estimated to be on the order of 10^5 particles per second. A weak indication of the $9/2_1^+ \rightarrow 5/2_1^+$ and $5/2_2^+ \rightarrow 7/2_1^+$ transitions, with energies of 1222 keV and 667 keV, respectively, are also indicated in the Sn Doppler corrected spectrum [17]. It was only possible to get an upper limit on their intensities. No significant de-excitation of the suggested single-neutron $3/2^+$ state at 1280 keV or the additional $3/2^+$ state at 1454 keV were observed in the experiment [9]. A level at 970 keV has been suggested to be a $3/2^+$ state [9] but was also not observed. The Ni intensity given in table 1 was used for normalization in the analysis discussed in detail below. The first excited 2^+ state in ^{58}Ni has a reduced transition probability of $B(E2; 0^+ \rightarrow 2^+) = 0.0704(15)\ e^2b^2$ [18].

The experimental data was analyzed using the semi-classical Coulomb excitation code GOSIA2 [19] to extract the $B(E2)$ value for the $5/2_1^+ \rightarrow 3/2_1^+$ transition. The Ni reduced matrix elements for the analysis were taken from ref. [18]. In ^{107}Sn, the excitation probability of the $3/2_1^+$ state may be effected by the excitation of other low-lying observed and unobserved states. Therefore, several additional states were included in the analysis. These include the $7/2_1^+$ state at 151 keV, the $5/2_2^+$ state at 818 keV, and the $9/2_1^+$ state at 1222 keV [17]. Our shell-model calculations, discussed below, predict a previously unobserved $7/2^+$ state in the region of 1400 keV. This state was also included in the analysis. The intensities used in the analysis for the two upper limits presented in table 1 may also have an effect on the $B(E2; 5/2_1^+ \rightarrow 3/2_1^+)$ value. These

Table 2. Sets of single-neutron orbits, given in MeV, used for the shell-model calculations described in the text.

Single-neutron orbit	SM A	SM B	SM C	SM D	SM E	SM F
$d_{5/2}$	0.0	0.0	0.0	0.0	0.0	0.172
$g_{7/2}$	0.172	0.172	0.172	0.172	0.172	0.0
$s_{1/2}$	1.55	2.45	2.2	1.6	2.6	2.3
$d_{3/2}$	1.66	2.54	2.3	2.0	2.7	2.5
$h_{11/2}$	3.55	3.0	2.7	2.3	3.4	3.4
Reference for $s_{1/2}, d_{3/2}, h_{11/2}$	[1]	[21]	[22]	[23]		

were not directly used as input to GOSIA2 but instead the calculated yields of these transitions were required to be lower than the limits given in table 1. The effects of these upper limits are discussed in further detail below.

The $E2$ and $M1$ matrix elements for the states used in the analysis were taken from the Shell-Model (SM F) calculations discussed in the following section. The standard neutron effective charge for the light Sn isotopes of $e_\nu = 1.0e$ [1] and the neutron g-factors, $g_l = 0$, $g_s = -3.82$ were used to generate the matrix elements. The known branching ratios for the levels at 704 keV and 818 keV were also included [17]. The $E2/M1$ mixing ratios for these states have not been measured previously. In the analysis, the $M1$ matrix elements and $E2$ matrix elements for the unobserved states along with the quadrupole moments of all states were fixed to the starting shell-model values.

The extracted transition probability is given in table 1. The error estimation procedure included in GOSIA2 does not account for correlations between the target and projectile matrix elements. The correlated error was therefore estimated by increasing and decreasing the $3/2_1^+ \rightarrow 5/2_1^+$ matrix element around the minimum value while allowing the $3/2_1^+ \rightarrow 7/2_1^+$ matrix element to reproduce the measured branching ratio and the Ni matrix elements to vary within their 1σ limits. The quoted error in table 1 corresponds to the $\chi^2{+}1$ limits.

Several tests were carried out to investigate the influence of the fixed shell-model matrix elements on the $B(E2; 5/2_1^+ \rightarrow 3/2_1^+)$ value. The matrix elements were varied coherently by $\pm 50\%$ and the minimization was repeated. The procedure is similar to previously published methods using the code GOSIA [20]. These changes only affected the measured $B(E2)$ value by a maximum of 0.003 e^2b^2. The matrix elements were also set to zero which decreased the reported value by 0.003 e^2b^2. In addition, the minimization was carried out using the SM E matrix elements, discussed below. This only affected the measured $B(E2)$ value by less than 0.001 e^2b^2. The best fit presented in table 1 predicted $\sim$10 counts to be present in both the $5/2_2^+ \rightarrow 7/2_1^+$ and Sn $9/2_1^+ \rightarrow 5/2_1^+$ transitions. To evaluate the influence of the measured upper limits, yields corresponding to the maximum values given in table 1 were used as input to GOSIA2. This resulted in an increase in the measured transition probability of 0.002 e^2b^2. The influence of the above tests are small compared to the quoted uncertainty in table 1.

4 Discussion

We have carried out a series of shell-model calculations to compare with the measured $B(E2)$ value. A set of effective two-body matrix elements and single-neutron orbits relative to ^{100}Sn make up the primary input to these calculations. The effective interaction used in this work was derived from a G-matrix renormalized CD-Bonn potential. This interaction has been frequently applied to the even-even Sn nuclei; see, for example, refs. [2,4]. Currently, the only available information for the single-neutron states in ^{101}Sn is the energy difference between the $d_{5/2}$ and $g_{7/2}$ orbits. We have therefore selected several sets of single-neutron energies to use in the calculations [1,21–23]. An important criterion for the selection was their close agreement with the experimentally determined energy splitting between the two lowest-lying orbits. In the calculations carried out in this work, the previously adopted value for the energy splitting has been replaced with the now measured value of 172 keV. The modified single-neutron orbits are shown in table 2 labeled SM A–SM D. The shell-model calculations, described in the following section, were also carried out using these sets with the inversion of the $d_{5/2}$ and $g_{7/2}$ orbits.

We have also fitted the single-neutron orbits in order to reproduce the suggested $s_{1/2}$ and $d_{3/2}$ single-neutron states and the low-lying $11/2^-$ state in ^{109}Sn [9,24]. This procedure was carried out for both selections of ground states in ^{101}Sn and the results are given as SM F and SM E in table 2. The search for the best sets was carried out by varying the single-neutron orbits in units of 1 MeV and locating the lowest chi-squared value calculated from the difference between the measured and calculated energies of these three states. The results of the fits for the excited states in ^{109}Sn are shown in panel B of fig. 2. The fits well reproduce the position of the single-neutron states. It can be noted that the calculations predict that the lowest $3/2^+$ state is the $d_{3/2}$ single-neutron state, based on the calculated occupation numbers. Previous experimental observations however suggest that the lowest-lying $3/2^+$ state is not the single-neutron state.

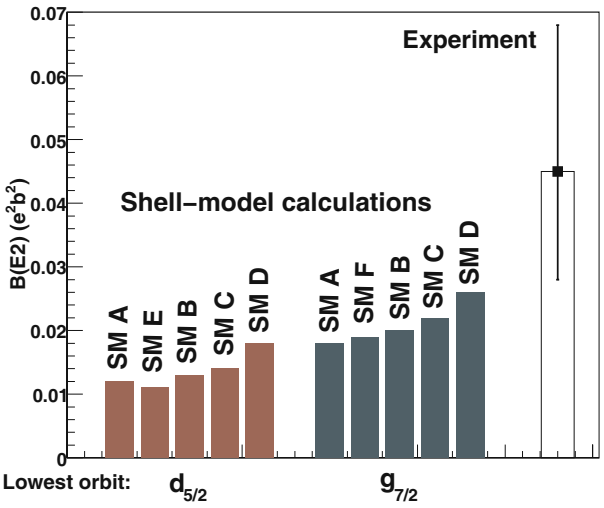

Fig. 3. Comparison between the measured and calculated $B(E2; 5/2_1^+ \rightarrow 3/2_1^+)$ values.

The calculated excited states in ^{107}Sn using the sets of single-neutron states in table 2 are shown in panel A of fig. 2. The bold markers indicate the three higher-lying single-neutron states based on the largest occupation numbers from our calculations. It is interesting to point out some features of these spectra. The SM A and SM D calculations predict low-lying single-neutron $1/2^+$ states, which have not been observed in previous experiments. This indicates that the energy of the orbit is too low in these calculations. On the other hand, since this state is difficult to populate in β-decay measurements [9] it is not possible to rule out its existence in this energy range. All the calculations, with the exception of SM A with the $d_{5/2}$ ground state, predict that the single-neutron $3/2^+$ state is not the lowest-lying $3/2^+$ state. This is in accordance with our measurement as the observation of the first $3/2^+$ state suggests that it cannot be the single-neutron state. The single-neutron states are expected to have small $B(E2)$ values and are thus less likely to be populated in Coulomb excitation.

The calculated transition probabilities for this state using the sets of single-neutron orbits are presented in fig. 3. Our measured value is also presented for comparison. All the shell-model values underestimate the measured value. Some of the missing strength can possibly be attributed to the inversion of the $d_{5/2}$ and $g_{7/2}$ orbits. In all cases, calculations with the $g_{7/2}$ orbit as the lowest-lying orbit produce an enhanced $B(E2)$ value with respect to the choice of the $d_{5/2}$ orbit as the lowest-lying orbit. The inversion of the orbits however worsens the agreement with the experimentally measured energy splitting between the $5/2^+$ and $7/2^+$ states in ^{109}Sn, as shown in fig. 2.

The three higher-lying orbits may also be important for the collectivity of the state. For instance, there is a correlation between the lowering of the energy of the $h_{11/2}$ orbit and the strength of the transition probability in fig. 3. We have verified this by setting the orbits energy to 2.3 MeV while fixing the energy of the other orbits to the SM F values. This resulted in an increase in the transition strength of $\sim 30\%$. Similarly, setting the energy of the $s_{1/2}$ state to 1.55 MeV and fixing the energies of the other orbits to the SM F values results in an increase of $\sim 10\%$ in the transition probability. Repeating the test with the $d_{3/2}$ energy set to 1.66 MeV however decreases the transition strength by $\sim 20\%$. A possible explanation is that the lowering of this orbit increases the single-neutron character of the lowest-lying $3/2^+$ state. It is therefore difficult to pinpoint the origin of the enhancement based on the energy of the single-neutron states alone. However, it is clear from our calculations that part of the missing strength may be explained by the ordering of the two lowest-lying orbits.

In ref. [6] it was found that good agreement with the energy splitting of the $5/2^+$ and $7/2^+$ states in the light Sn nuclei could be achieved with the $d_{5/2}$ orbit as the lowest-lying single-neutron orbit relative to ^{100}Sn if the $(g_{7/2})^2_{0^+}$ matrix element was reduced by $\sim 20\%$. In order to explore the effect of this matrix element on the reduced transition probability in ^{107}Sn, we carried out a shell-model calculation using the SM E set and a 20% reduced $(g_{7/2})^2_{0^+}$ matrix element. We found that this leads to an $\sim 30\%$ reduction of the calculated $B(E2)$ value.

Another explanation for the missing transition strength could be related to core excitations of neutrons and protons across the shell gap, as discussed previously [1–4]. In recent shell-model calculations in ^{98}Cd, a $5/2^+$ ground state was predicted in ^{101}Sn with the inclusion of neutron excitations across the $N = 50$ shell gap [25]. Interestingly, the calculations predicted a $7/2^+$ ground state when the core excitations were not included.

To compliment the shell-model calculations presented here, we have also analyzed the measured $B(E2)$ value under the framework of the simple core-excitation model [26]. In the model, the low-lying excited states of ^{107}Sn can be described by the coupling of a single-neutron to an excited 2^+ core. The $B(E2)$ strength of the core is expected to be distributed amongst the core-coupled multiplet. Under the assumption that the core has the same properties as ^{106}Sn, with $B(E2; 0^+ \rightarrow 2^+) = 0.195(39)\ e^2b^2$ [4], the model predicts for ^{107}Sn a reduced transition probability of $B(E2; 5/2_1^+ \rightarrow 3/2_1^+) = 0.026(5)\ e^2b^2$. It may thus be concluded that the simple coupling scheme underestimates the amount of core polarization in ^{107}Sn.

5 Summary

In summary, we have presented the first measurements of the transition strength for the lowest-lying $3/2^+$ state in the neutron-deficient isotope ^{107}Sn. This is the lightest odd-Sn nucleus measured using Coulomb excitation to this date. The measured transition strength is enhanced with respect to state-of-the-art shell-model calculations. One potential source of the missing strength is the ordering of the two lowest-lying single-neutron orbits relative to ^{100}Sn. In all our calculations, the strength is enhanced

with the $g_{7/2}$ orbit as the lowest-lying orbit compared to when the $d_{5/2}$ state is the lowest orbit. In addition, we have shown that the position of the three higher-lying orbits contribute to some extent to the collectivity of the observed state. These results further emphasize the need for firm experimental evidence of the single-neutron dominated states relative to ^{100}Sn.

This work was supported by the Swedish Research Council, the European Union under Contract RII3-EURONS 506065 and the German BMBF under Contract No. 06KY9136I. JD would like to acknowledge the support of FWO-Vlaanderen (Belgium).

Open Access This is an open access article distributed under the terms of the Creative Commons Attribution License (http://creativecommons.org/licenses/by/3.0), which permits unrestricted use, distribution, and reproduction in any medium, provided the original work is properly cited.

References

1. A. Banu *et al.*, Phys. Rev. C **72**, 061305(R) (2005).
2. J. Cederkäll *et al.*, Phys. Rev. Lett. **98**, 172501 (2007).
3. C. Vaman *et al.*, Phys. Rev. Lett. **99**, 162501 (2007).
4. A. Ekström *et al.*, Phys. Rev. Lett. **101**, 012502 (2008).
5. W.K. Dagenhart *et al.*, Nucl. Phys. A **284**, 484 (1977).
6. D. Seweryniak *et al.*, Phys. Rev. Lett. **99**, 022504 (2007).
7. I.G. Darby *et al.*, Phys. Rev. Lett. **105**, 162502 (2010).
8. J. Blachot, Nucl. Data Sheets **110**, 1239 (2009).
9. J.J. Ressler *et al.*, Phys. Rev. C **65**, 044330 (2002).
10. I. Dankó *et al.*, Nucl. Phys. A **646**, 3 (1999).
11. A. Jungclaus *et al.*, Phys. Lett. B **695**, 110 (2011).
12. O. Kester *et al.*, Nucl. Instrum. Methods Phys. Res. B **204**, 20 (2003).
13. F. Ames *et al.*, Nucl. Instrum. Methods Phys. Res. A **538**, 17 (2005).
14. F. Wenander *et al.*, Nucl. Phys. A **701**, 528 (2002).
15. P. Reiter *et al.*, Nucl. Phys. A **701**, 209 (2002).
16. A.N. Ostrowski *et al.*, Nucl. Instrum. Methods Phys. Res. A **480**, 448 (2002).
17. J. Blachot, Nucl. Data Sheets **109**, 1383 (2008).
18. C.D. Nesaraja *et al.*, Nucl. Data Sheets **111**, 897 (2010).
19. T. Czosnyka *et al.*, Bull. Am. Phys. Soc. **28**, 745 (1983).
20. M.A. Schumaker *et al.*, Phys. Rev. C **78**, 044321 (2008).
21. T. Engeland *et al.*, Phys. Scr. T **56**, 58 (1995).
22. F. Andreozzi *et al.*, Phys. Rev. C **54**, 1636 (1996).
23. C. Fahlander *et al.*, Phys. Rev. C **63**, 021307(R) (2001).
24. J. Blachot, Nucl. Data Sheets **107**, 355 (2006).
25. A. Blazhev *et al.*, J. Phys. Conf. Ser. **205**, 012035 (2010).
26. A. de-Shalit, Phys. Rev. **122**, 1530 (1961).